

SAND99-0399C

# SOLUTION MINING RESEARCH INSTITUTE

3336 Lone Hill Lane  
Encinitas, CA 92024-7262  
619-759-7532

MEETING  
PAPER



## CORRELATION OF CREEP BEHAVIOR OF DOMAL SALTS

by

Darrell E. Munson  
Sandia National Laboratories, Albuquerque, NM 87185

Prepared for

Spring Meeting  
Solution Mining Research Institute  
April 14-16, 1999  
Las Vegas, Nevada

# CORRELATION OF CREEP BEHAVIOR OF DOMAL SALTS

Darrell E. Munson  
Sandia National Laboratories, Albuquerque, NM 87185\*

## ABSTRACT

The experimentally determined creep responses of a number of domal salts have been reported in the literature. Some of these creep results were obtained using standard (conventional) creep tests. However, more typically, the creep data have come from multistage creep tests, where the number of specimens available for testing was small. An incremental test uses abrupt changes in stress and temperature to produce several time increments (stages) of different creep conditions. Clearly, the ability to analyze these limited data and to correlate them with each other could be of considerable potential value in establishing the mechanical characteristics of salt domes, both generally and specifically. In any analysis, it is necessary to have a framework of rules to provide consistency. The basis for the framework is the Multimechanism-Deformation (M-D) constitutive model. This model utilizes considerable general knowledge of material creep deformation to supplement specific knowledge of the material response of salt. Because the creep of salt is controlled by just a few micromechanical mechanisms, regardless of the origin of the salt, certain of the material parameters are values that can be considered universal to salt. Actual data analysis utilizes the methodology developed for the Waste Isolation Pilot Plant (WIPP) program, and the response of a bedded pure WIPP salt as the baseline for comparison of the domal salts. Creep data from Weeks Island, Bryan Mound, West Hackberry, Bayou Choctaw, and Big Hill salt domes, which are all sites of Strategic Petroleum Reserve (SPR) storage caverns, were analyzed, as were data from the Avery Island, Moss Bluff, and Jennings salt domes. The analysis permits the parameter value sets for the domal salts to be determined in terms of the M-D model with various degrees of completeness. In turn this permits detailed numerical calculations simulating cavern response. Where the set is incomplete because of the sparse database, reasonable assumptions permit the set to be completed. From the analysis, two distinct response groups were evident, with the salts of one group measurably more creep resistant than the other group. Interestingly, these groups correspond well with the indirectly determined creep closure of the SPR storage caverns, a correlation that probably should be expected. Certainly, the results suggest a simple laboratory determination of the creep characteristics of a salt material from a dome site can indicate the relative behavior of any potential cavern placed within that dome.

---

\*Sandia is a multiprogram laboratory operated by Sandia Corporation, a Lockheed Martin Company, for the U. S. Department of Energy under Contract DE-AC04-94AL5000.

## **DISCLAIMER**

This report was prepared as an account of work sponsored by an agency of the United States Government. Neither the United States Government nor any agency thereof, nor any of their employees, make any warranty, express or implied, or assumes any legal liability or responsibility for the accuracy, completeness, or usefulness of any information, apparatus, product, or process disclosed, or represents that its use would not infringe privately owned rights. Reference herein to any specific commercial product, process, or service by trade name, trademark, manufacturer, or otherwise does not necessarily constitute or imply its endorsement, recommendation, or favoring by the United States Government or any agency thereof. The views and opinions of authors expressed herein do not necessarily state or reflect those of the United States Government or any agency thereof.

## INTRODUCTION

In recent years, several significant technical developments have been made in the areas of salt mechanics and salt cavern operation that can be applied advantageously to an improved analysis of salt creep behavior of domal salts. Results of such analysis can potentially be useful in the better selection, construction, and operation of future caverns in salt domes. The relevant developments are the accumulation of laboratory creep databases for a relatively large number of domal salts, formulation of a general constitutive model, and collection of field data on the relative volume loss in existing caverns with time.

Creep databases have been reported for a number of salt dome materials, with the largest contribution from salt domes of the Strategic Petroleum Reserve (SPR) cavern facilities. The SPR sites are located in the Weeks Island, Bayou Choctaw, and West Hackberry domes in Louisiana and the Bryan Mound and Big Hill domes in Texas. Early creep tests were performed by Wawersik, et al. [1980a] on material from the Bryan Mound site and by Wawersik, et al. [1980b] on material from the West Hackberry site. Later, Wawersik and Zeuch [1984] performed multistage tests on core specimens from Bryan Mound, West Hackberry, and Bayou Choctaw domes. Wawersik [1985] completed the early studies of the SPR site domes by testing Big Hill specimens. Recently, using standard (conventional) test procedures, creep tests were performed on specimens obtained from borehole cores of the Weeks Island salt dome [Mellegard and Pfeifle, 1996], which contains an underground mine used for SPR storage. Creep results have been reported for domal salts from other sites as well, specifically from the Avery Island [DeVries, 1988], Moss Bluff [Wawersik, 1992], and Jennings [Wawersik and Zimmerer, 1994] domes. Specimens prepared from these salt materials were tested according to acceptable creep testing methods of that time. Often, to maximize information and minimize testing time, this involved multistage testing methods with numerous changes of stress and temperature during the creep deformation of an individual specimen. Even though multistage tests differ significantly from standard creep tests, most of these multistage creep-testing methods contain information compatible with the test methods developed for the Waste Isolation Pilot Plant (WIPP) program [Munson, et al., 1989]. These methods have been applied to determine parameter sets for the salt materials obtained from bedded salt layers of the WIPP facility. While the individual creep tests on the domal salts were analyzed when reported by the original investigators, apparently no subsequent comprehensive analysis of the collective database is available, except for a statistical analysis by Pfeifle, et al. [1996] to obtain correlation coefficients for several diverse parameters. Although the material databases are significant, they are not necessarily sufficient for complete parameter evaluation according to the WIPP analysis methodology. Nevertheless, various degrees of partial parameter evaluations are possible.

In the work presented here, the mathematical framework for the Multimechanism Deformation (M-D) model of salt creep is developed to support the method and requirements for parameter evaluation. On this basis, either full or partial parameter sets for each individual dome material are determined from the data and from comparisons with the complete parameter set from the WIPP clean salt database. From these comparisons, one group of domal salts has a steady state creep behavior essentially the same as WIPP clean salt, while another group of domal salts creep much slower than the WIPP salt. This difference between domal salt response has been suggested previously because of the low steady-state creep rates of Bryan Mound salt [Wawersik, et al., 1980a] compared to other domal salts, but the effect was not quantified to the extent possible here. The results of the analyses are compared to the volume creep rate of the SPR caverns as measured by the CAVEMAN analysis of the historical pressurization data [Ehgartner, et al., 1995]. This comparison suggests that the steady state creep rate and the volume creep response are correlated. The work concludes with a brief summary.

## ANALYSIS METHOD

A standard creep test is one in which the specimen strain is measured as a function of time for imposed conditions of constant uniaxial stress and constant temperature. For geotechnical applications, the uniaxial stress is typically replaced by a triaxial compression stress condition, which suppresses fracture in geomaterials and more accurately duplicates the natural conditions around underground openings. Standard creep tests produce most directly the transient and steady state response of the material being tested. However, standard creep tests are time consuming and costly. This has led some investigators to utilize “staged” tests in an attempt to increase data retrieval from a single specimen. (Henceforth, we use “incremental” rather than “staged” as the descriptive terminology for these tests to avoid confusion with historical descriptions of the three stages of creep behavior). Normally for geologic materials, incremental tests are triaxial compression tests in which either the stress or temperature, or both, are changed periodically in a step-wise fashion to give small time increments of creep at constant stress and temperature, all upon the same specimen. Using the concept of a transient creep curve [Munson and Dawson, 1982], the implications of these incremental stress and temperature changes can be examined and compared to the standard creep test. An example of a typical standard test, showing both axial and radial strains, for the creep of salt from the Weeks Island dome appears in Figure 1.

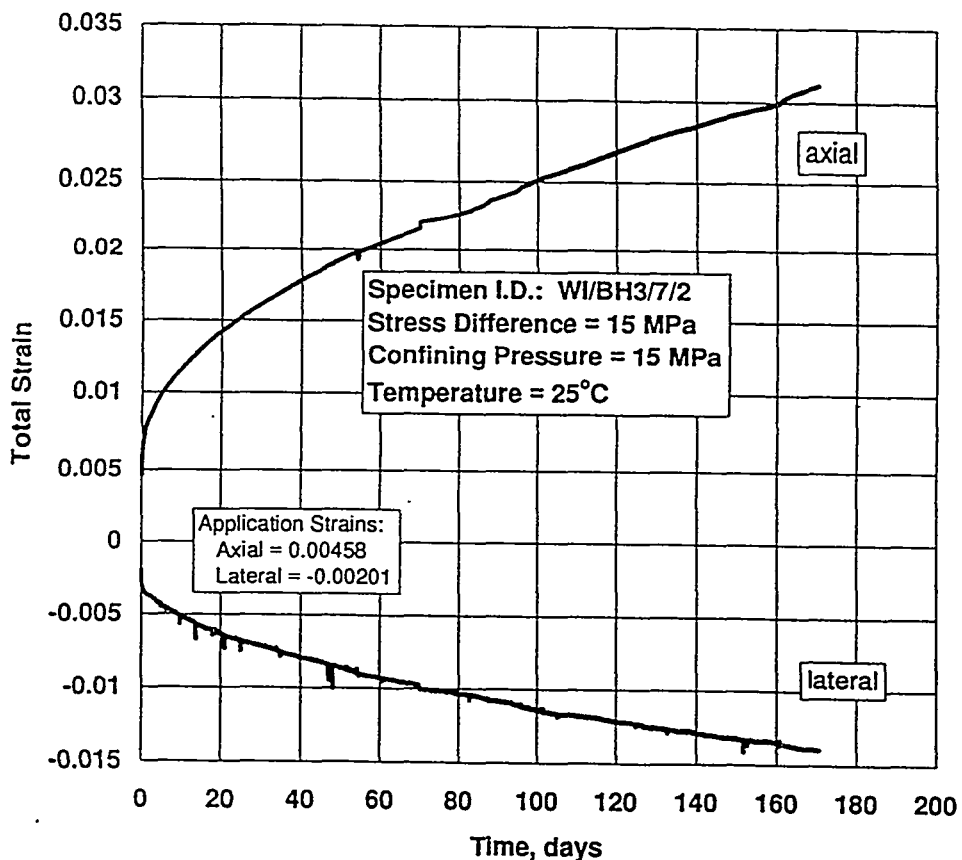


Figure 1. Raw Creep Curve for Weeks Island Salt [after Mellegard and Pfeifle, 1996].

While the standard creep curve appears straightforward, this is not the case. Unfortunately, from raw creep results it is relatively easy to misinterpret the relevant behavior. However, if the derivative of the strain with respect to time (instantaneous strain rate) is determined and then plotted against time, the curve of Figure 2 is produced. This plot indicates that the strain rate diminishes with time, to eventually asymptote to a steady state (constant) rate. While there can still be uncertainty in determining the exact asymptote in Figure 2, the resulting achievement of steady state is clearly more apparent than from the raw data curve. Now, in order to understand the creep response in even greater detail, it is necessary to further reframe the plot of Figure 2. This is accomplished by visualizing the creep strain as involving two components, one produced by a steady state creep rate and one produced by a transient creep rate. We can effectively separate these strains by using the steady state rate to normalize the instantaneous strain rate and by introducing an internal state parameter,  $\zeta$ , which is a measure of the transient strain. But, in contrast to the creep strain, which increases monotonically, the internal state parameter value may either increase or decrease in transient creep, yet remains constant in steady state creep. The plot of normalized instantaneous strain rate against the internal state parameter provides a significant insight into creep, especially when the plot includes both workhardening and recovery branches.

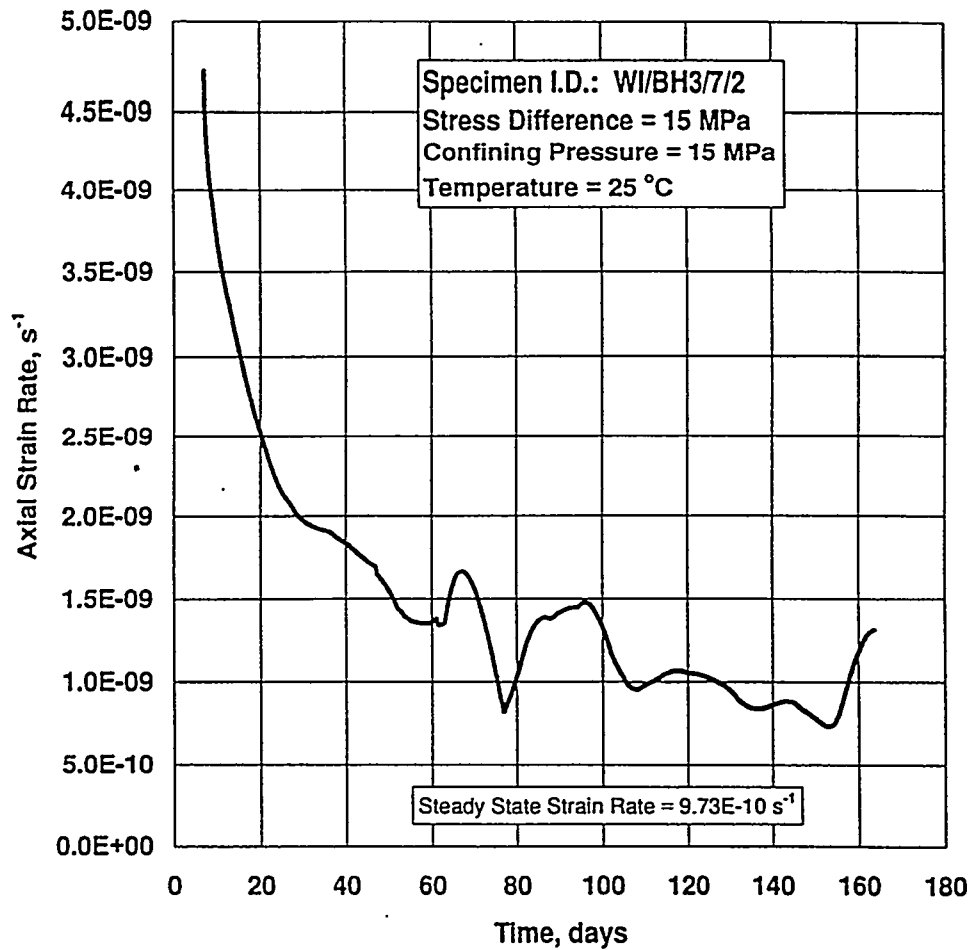


Figure 2. Axial Strain Rate Asymptote to Steady State [after Mellegard and Pfeifle, 1996].

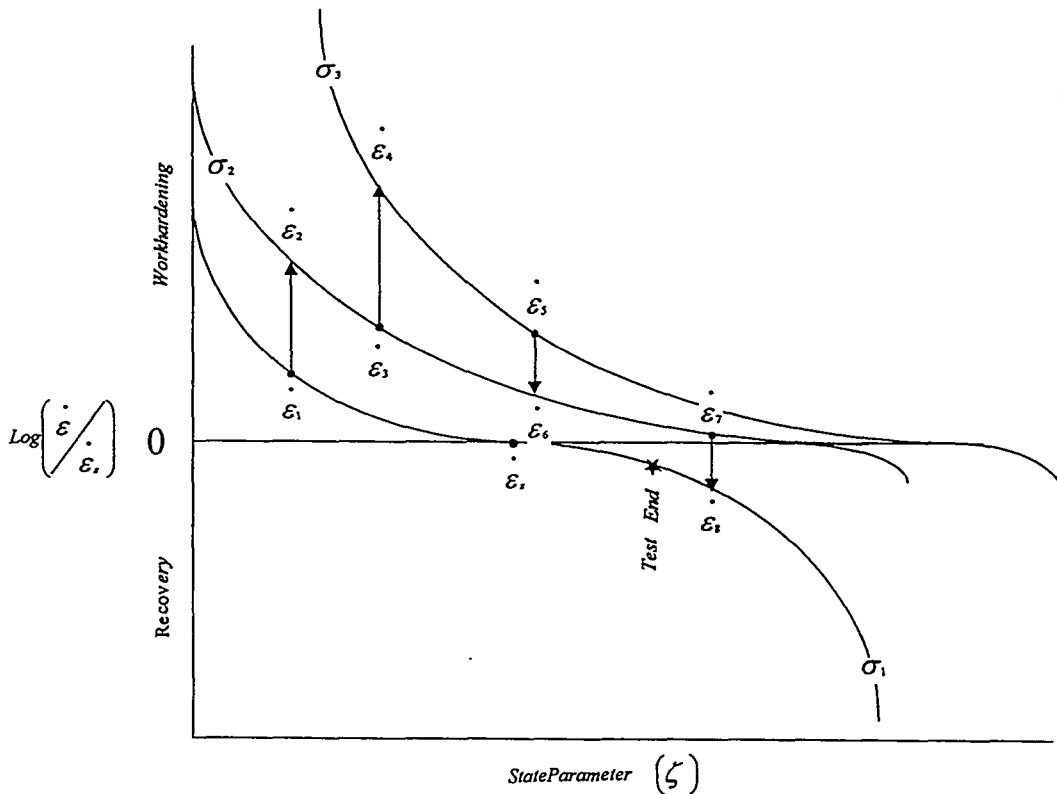


Figure 3. Transient Creep Curves for Various Stresses [after Munson and Dawson, 1982].

This curve, as shown in Figure 3, is called the “transient creep curve.” Actually it is a family of transient creep curves for various constant applied stresses [Munson and Dawson, 1982]. At any given initial applied stress, for example  $\sigma_1$ , the strain rate of an initially undeformed specimen decreases with time, or with increases in the internal state parameter,  $\zeta$ , until the strain rate becomes the equilibrium or steady state strain rate. At this point, marked as  $\dot{\epsilon}_s$  on the  $\sigma_1$  transient strain curve, the strain rate and internal state parameter will remain constant. Significantly, for a specimen that is initially workhardened, the current state parameter value may be greater than the state parameter value at steady state, i.e., to the right of the steady state point on the  $\sigma_1$  transient strain curve. With time, the state parameter of this specimen will decrease and, although the specimen strain and strain rate continues to increase, the state of the material will move backward up the transient curve, to eventually attain the steady state condition. The strain rate will then again become constant. This behavior is expressed mathematically through a constitutive model of creep.

Transient strain curves were proposed by Munson and Dawson [1982] as a strategy to treat transient creep during stress and temperature changes. While, many different scenarios are possible based on the actual tests, one hypothetical series of stress increases and stress decreases such as might be generated in an incremental test are illustrated in Figure 3. The strain rate history for each increment can be deduced from the figure, where directions of the incremental changes in stress are given by the arrows. Tracing these changes in the figure shows that after the specimen is initially loaded under  $\sigma_1$ , an interval of decreasing transient strain rate occurs. The stress is then increased to  $\sigma_2$ , with the subsequent abrupt increase in strain rate followed by a decreasing transient strain rate. After an interval of time, the stress is further raised to  $\sigma_3$ . Note that the strain

rates at each higher stress level still diminish with time, as one would expect, but they never become steady state rates. From  $\sigma_3$ , the stress is lowered to  $\sigma_2$ , and while the rate decreases, it is still not in steady state by the time the stress is again further reduced to  $\sigma_1$ . However, this last stress decrease causes an unusually strong decrease in strain rate since the specimen internal state is now on a recovery branch. If we use final strain rates as is customarily reported for each of the increments, and exactly as was done for the incremental tests on the domal salts, then we will have four rates above the steady state rate and one below the steady state rate. None of the final strain rates, however will actually be the steady state rate, although one will be close. The crucial problem with incremental test data is that we usually do not know the steady state rate or how the reported rates are related to steady state.

In the following discussion of the analysis, as well as the actual analysis of the creep data, we want to keep the details of Figure 3 in our minds. This illustration is the clearest possible method of keeping track of the complex series of events during any incremental creep test.

### MODEL FRAMEWORK

In addition to the empirical observations, as described above, it is equally possible, and perhaps more important, to make use of what is known about the general constitutive behavior of salt in order to formulate an analysis strategy [Munson, et al., 1989]. Not only do the constitutive equations of the M-D model define the necessary material parameters, but also they permit the formulation of principles or rules of the analysis. In developing the constitutive description, we concern ourselves only with the temperature and stress range encountered in mining and storage cavern operations, typically low temperature and low to moderately high stresses. For these conditions, the creep is envisioned as arising from the contributions of three appropriate micromechanical mechanisms as determined from the deformation mechanism-map [Munson, 1979]. These mechanisms are (1) a dislocation climb controlled creep mechanism at high temperatures and low stresses, (2) an empirically specified but undefined mechanism at low temperatures and low stresses, and (3) a dislocation slip controlled mechanism at high stresses [Munson, et al., 1989]. The respective steady state creep rates for the three individual mechanisms are given by:

$$\dot{\epsilon}_{s_1} = A_1 e^{\frac{-Q_1}{RT}} \left( \frac{\sigma}{\mu(1-\omega)} \right)^{n_1}$$

$$\dot{\epsilon}_{s_2} = A_2 e^{\frac{-Q_2}{RT}} \left( \frac{\sigma}{\mu(1-\omega)} \right)^{n_2}$$

1

$$\dot{\epsilon}_{s_3} = \left| H(\sigma - \sigma_0) \left( B_1 e^{\frac{-Q_1}{RT}} + B_2 e^{\frac{-Q_2}{RT}} \right) \sinh \left[ \frac{q \left( \frac{\sigma}{1-\omega} - \sigma_0 \right)}{\mu} \right] \right|$$

where the numerical subscripts refer to the appropriate mechanism, the A's and B's are structure factors, Q's are activation energies, R is the universal gas constant, T is the absolute temperature,  $\mu$  is the shear modulus, q is the stress constant,  $\sigma_0$  is a stress limit, and H is a Heaviside step



function with argument  $(\sigma - \sigma_0)$ . It has been shown [Munson, et al., 1989] through multiaxial experiments that the proper flow law, or equivalent stress measure, is  $\sigma = |\sigma_1 - \sigma_3|$ .

These mechanisms act in parallel, which means the individual steady state creep rates can be summed over the three mechanisms to give the total steady state creep rate, as follows:

$$\dot{\varepsilon}_s = \sum_{i=1}^3 \dot{\varepsilon}_{s_i} \quad 2$$

The equivalent total strain rate is treated through a multiplier on the steady state rate, as

$$\dot{\varepsilon}_{eq} = F \dot{\varepsilon}_s \quad 3$$

where the multiplier involves three branches of the transient creep curve: workhardening, steady state, and recovery, respectively, as follows:

$$F = \begin{cases} e^{\Delta \left( \left( 1 - \frac{\zeta}{\varepsilon_i^*} \right)^2 \right)} & ; \zeta < \varepsilon_i^* \\ 1 & ; \zeta = \varepsilon_i^* \\ e^{-\delta \left( \left( 1 - \frac{\zeta}{\varepsilon_i^*} \right)^2 \right)} & ; \zeta > \varepsilon_i^* \end{cases} \quad 4$$

Here,  $\Delta$  is the workhardening parameter,  $\delta$  is the recovery parameter,  $\zeta$  is the state parameter, and  $\varepsilon_i^*$  is the transient strain limit. The kinetic equation for the state parameter is given by

$$\dot{\zeta} = (F - 1) \dot{\varepsilon}_s \quad 5$$

The transient strain limit is defined by

$$\varepsilon_i^* = K_0 e^{c\tau} \left( \frac{\sigma}{\mu(1-\omega)} \right)^m \quad 6$$

where  $K_0$  and  $c$  are constants and  $m$  is a material constant.

The workhardening,  $\Delta$ , and recovery,  $\delta$ , parameters are described through linear functions, as follows:

$$\Delta = \alpha_w + \beta_w \log\left(\frac{\sigma}{\mu(1-\omega)}\right)$$

$$\delta = \alpha_r + \beta_r \log\left(\frac{\sigma}{\mu(1-\omega)}\right)$$

7

where the  $\alpha$ 's and  $\beta$ 's are constants. Throughout these equations, although it is taken as zero for our purposes here,  $\omega$  is the damage parameter. All total, there are 17 parameters to be evaluated, not counting the damage parameter and the elastic constants. However, a number of the parameters are obtained from "outside" physical processes, as will be discussed later.

Based on the constitutive equations and expected limits of behavior, the governing principles of the analysis are:

(1) Because all creep is controlled by the same micromechanical mechanisms, Eq. 1 and Eqs. 2 define the shape of the steady state creep response with stress. As a result, *differences in the steady state response of different materials will be reflected as changes in the values of those parameters that are not fixed by other considerations.*

(2) Eq. 4 is the mathematical representation of the transient strain curves depicted graphically in Figure 3, which produces a family of curves in stress. Moreover, the steady state strain rate always increases as the stress is increased, as determined from the steady state equations for the three mechanisms in Eqs. 2. In addition, the absolute strain value of the state parameter at steady state creep, which is the transient strain limit given by Eq. 6, increases as the stress increases. Thus, it can be determined that all of the possible transient strain and strain rate states for any increments of progressively increasing stress are above and to the left of the steady state condition in Figure 3. Therefore, just as the limit of any individual transient creep curve is the steady state creep rate, the limit of creep along all of the family of curves is a steady state creep condition so long as the stress changes progressively increase. Thus, we can state as a general principle, *the lower bound of the collection of creep rates of incremental tests where the stress changes are always to progressively higher stresses tends toward (approaches) the steady state creep rate as a function of stress.*

(3) Decreases in the stress during incremental tests may result in moving to a new transient strain curve either above or below the steady state creep rate. Unless the duration of the increment is long, one may not know with any certainty whether the creep rate is decreasing or increasing; i.e., whether steady state rate is being approached from above (workhardening) or below (recovery) in Figure 3. As a result, *creep rates measured after a stress decrease generally may be difficult to interpret and, in this analysis, increments after a stress drop are ignored.*

(4) Temperature changes normally will not cause interpretation difficulties, except when a *temperature decrease* occurs when a specimen is very near or in steady state creep or when the *temperature decrease* is marked. Thus, *one must be careful when utilizing data from temperature decreases to assure that the change does not induce a recovery condition.*

Fundamentally, salt creep behavior has common micromechanical constitutive features regardless of the origin of the salt, all that differs is the exact value of the parameters. In particular, those critical parameters that primarily distinguish one salt material from another salt material are the steady state responses as represented by the structure factors (A's and B's) and the transient strain rate limits ( $\epsilon^*$ ) as represented by  $K_0$ . Although not a critical parameter,  $\Delta$  may also be material sensitive. By using the analysis criteria given above and the known behavior from the well-documented tests for a WIPP "clean" salt (99.5+% NaCl) as a baseline response, it may be

possible on the one hand to construct reasonable steady state responses for the domal salts. On the other hand, determination of the transient strain limit depends critically upon having the complete transient strain curves, i.e., complete conventional raw creep curves. In the absence of these curves, only uncertain estimates can be made for values for this parameter. Remaining parameters are either unaffected by or insensitive to the specific salt material.

Some comment is necessary on the nature of the bound determined from incremental test data. This is a consequence of the fact that any bound formed by incremental data alone may be still well removed from the actual steady state response. The uncertainty is such that the apparent bound will always be greater than the actual steady state response. Consequently, when the construction of the steady state response involves a series of tests that include both incremental and standard tests, the standard tests will be the dominant data in the determination. When the database is solely composed of incremental test data, caution must be used.

## DOMAL SALTS RESULTS

In presenting the analysis of the reported data, we begin with Weeks Island (WI) and Avery Island (AI) salts because they represent the most complete data collections in terms of standard creep tests. The analysis for the M-D model is direct and the results can be compared extensively to the WIPP clean salt baseline. Then the remaining salt dome data are analyzed and compared to the extent possible to the WIPP clean salt baseline data.

### WEEKS ISLAND AND AVERY ISLAND

The Weeks Island (WI) salt dome petroleum storage is underground in the rooms and drifts of an salt mine previously operated in the dome and purchased for the SPR. The salt was cored through shallow boreholes from the ground surface into the salt at several locations in the dome. Grain diameters were locally uniform, but varied from location to location, ranging from 3.7 to 12.7 mm (0.12 to 0.5 inches). The salt was unusually pure with a principal impurity content of 1 to 2%, consisting almost entirely of anhydrite [Ortiz, 1980]. The dome is thought to have several splines separated by shear zones [Neal, et al., 1993a]. These zones are apparent in the mine, primarily through concentrations of impurities in the shear zones between splines.

Recently Mellegard and Pfeifle [1996] tested four specimens of Weeks Island salt prepared from material taken from Well No. BH-3. The borehole was not especially deep, reaching from the ground surface just into the salt. Even though a limited number of tests were made, procedures used were designed to characterize nearly all of the nonthermal parameters of the second mechanism of the M-D model of creep (the exception is the recovery parameter). In addition the strains produced by the application of the axial load were measured and reported. Although not important for determining the steady state creep response, application strains have a bearing on evaluation of transient creep parameters.

As discussed previously, a steady state condition was determine from the first derivative of the raw data (creep rate) plotted as a function of time, as shown in Figure 2. Either a smoothed visual or exponential curve fitted to the experimental data of Figure 2 gives an asymptotic steady state rate of about  $9.73 \times 10^{-10}$  /s. Steady state creep rates from the four creep tests are plotted in logarithmic form against the creep stress in Figure 4. The slope of the data is just the parameter  $n_2$ , while the intercept of the line on the ordinate axis is the structure parameter,  $A_2$ . Basically, the structure factors for the other two mechanisms are determined similarly, when there are sufficient data to do so. In our case, since there are insufficient data to determine the other structure factors, we will

assume that all structure factors change in the same proportion as the ratio of  $A_2$  compared to the WIPP clean salt baseline.

In Figure 4, Weeks Island domal salt steady state creep data at 22°C are compared to the more extensive data from clean WIPP bedded salt, both with about the same impurity content. The solid line in the figure is actually determined from an even more extensive creep database and from the

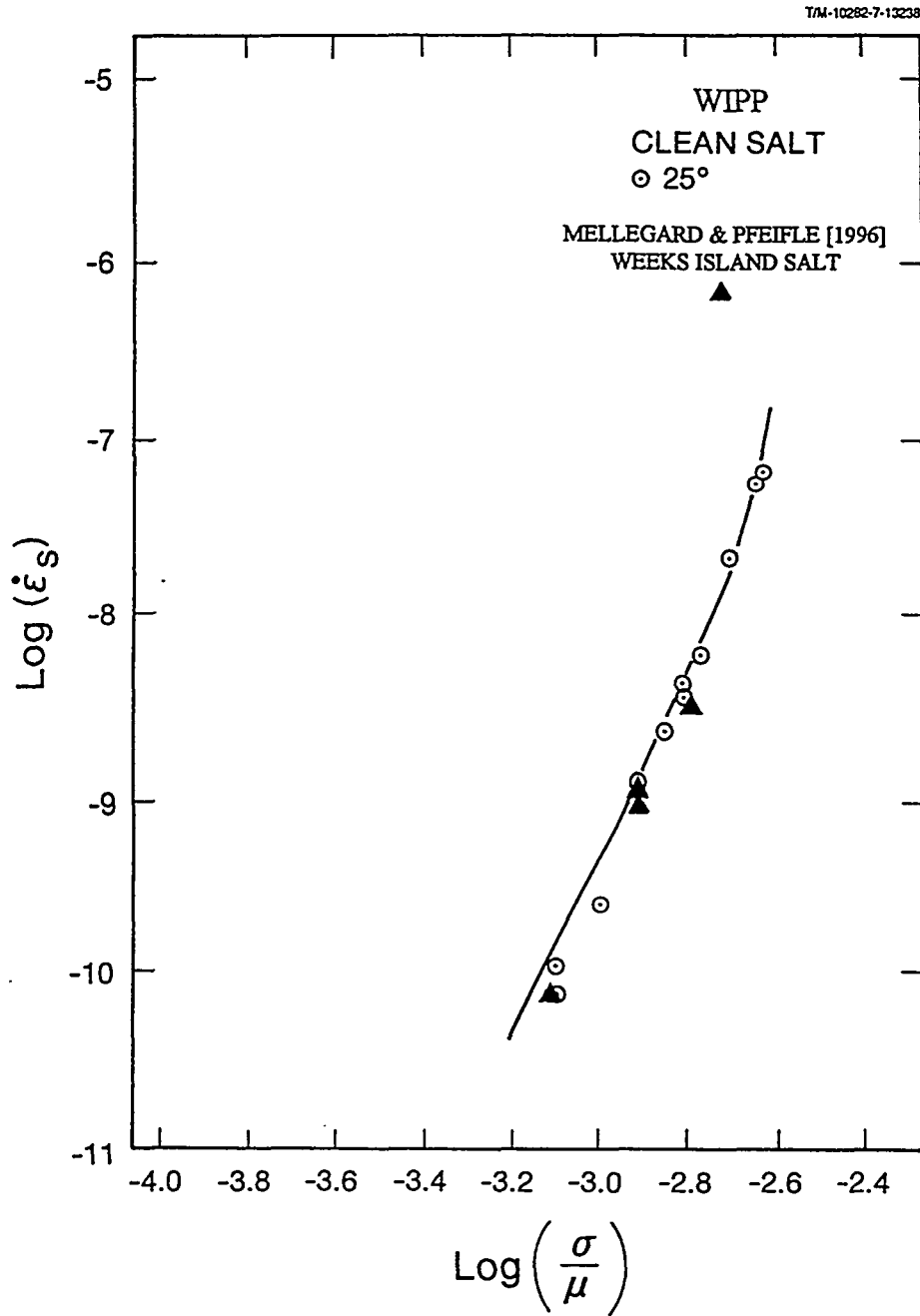


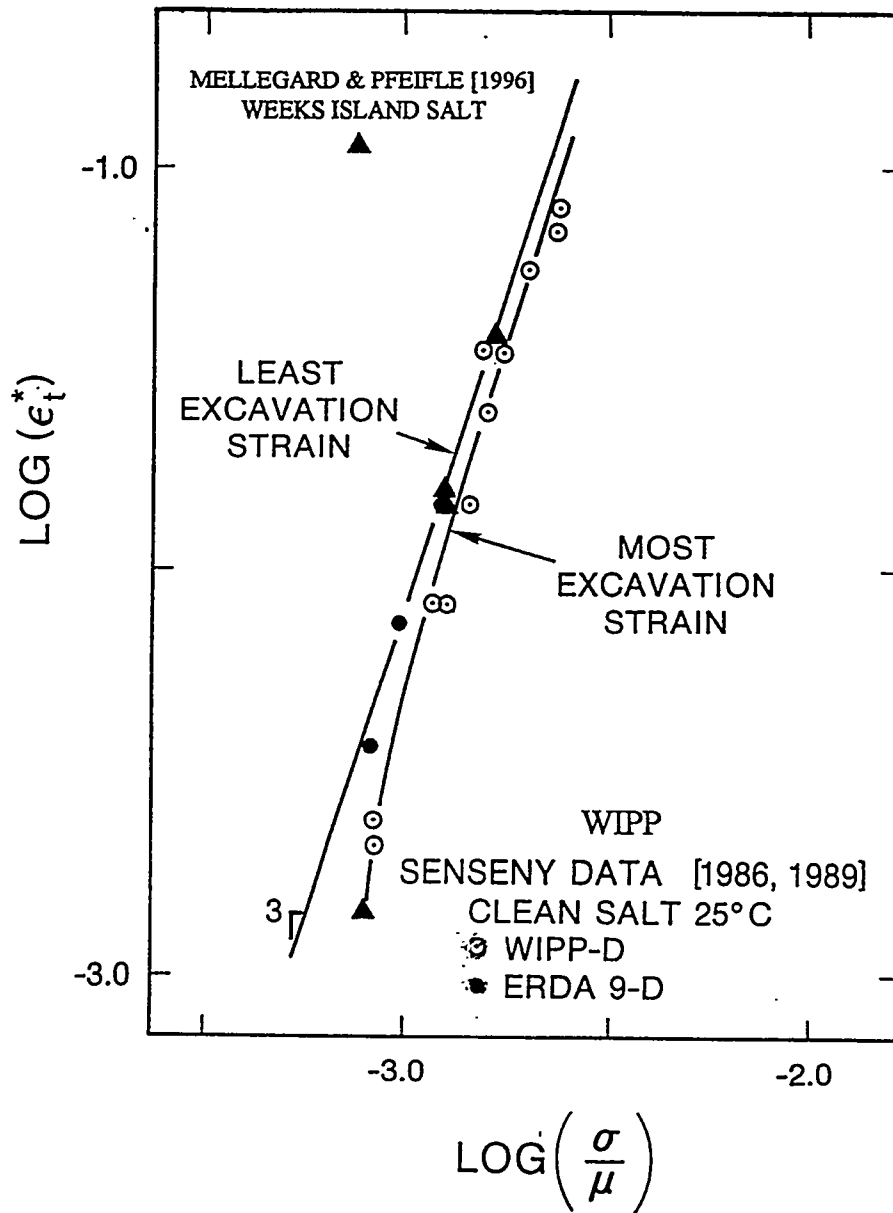
Figure 4. Steady state response of Weeks Island and WIPP salt [Munson and Ehgartner, 1997].

independent inputs from micromechanical models that were used to establish the form and slope of the curve for the two mechanisms controlling salt creep for these conditions [Munson, et al., 1989]. The third mechanism dominant at higher temperatures is not normally involved here. As is apparent, Weeks Island data are very comparable to the WIPP data, except that they are offset vertically, by a factor of about 0.50 (log -0.30), resulting in a smaller structure factor value. However, when we consider the difference because of the temperature, 22°C vs. 25°C, this itself causes a shift by a factor of 0.84 (log -0.0746). Therefore, the net offset due to the difference in materials is only a factor of 0.59 (log -0.23).

Although the values of the model constants given by Munson, et al. [1989] are independent of both stress and temperature, they are not independent of those affects due to differences in material. However, whether or not the influence of temperature can be observed depends upon how the data are presented. Consequently, in plots such as Figure 4 for the same material, the different temperatures will cause a shift to produce a family of curves all with similar characteristics, but offset from each other. Specifically, in the logarithmic plots that we are using here, differences caused by temperature will manifest themselves as a change in intercept on the ordinate. Again, this observed temperature induced change does not translate into an actual change in the structure factors. On the other hand, however, in these plots, material differences also appear as differences in the value of the intercept, which must be interpreted as a real difference in the value of structure factor,  $A$ . In order to determine the material affect, it is necessary to reduce the observed responses obtained in these plots of creep data to an equivalent response at 25°C. Then, any difference between the reduced response and the WIPP clean salt response at 25°C will be a true difference caused entirely by the material. It is generally believed [Munson, et al., 1989] that the uncertainty in an individual steady state creep rate determination is about a factor of two, or a log difference of +/- 0.30. Within this uncertainty, any of the Weeks Island data points would be indistinguishable from the WIPP data. However, as more data are considered, the nature of the uncertainty changes. Thus, the best-fit line to a collection of data does not have an uncertainty as large as a single datum. Even with the small amount of Weeks Island data presented here, the creep rates are all uniformly lower than the best representation of the WIPP data. As a consequence, we believe the steady state rate of Weeks Island salt to be measurably less, although not much less, than WIPP clean salt.

Once the steady state creep rate has been determined for a given test, then Figure 1 can be used to determine a transient strain limit,  $\epsilon^*_t$ . A line with the steady state slope is constructed asymptotic to the creep curve on the raw creep curve and the intercept of this line on the ordinate (strain) axis gives the transient strain limit for that test. When these transient strain limit values are plotted in Figure 5 as a function of stress, the behavior appears essentially identical to that of the WIPP clean salt baseline. The intercept of the line with slope  $m$  in Figure 5 on the ordinate gives the value of the parameter  $K_0$ . This means that the  $K_0$  parameter value for Weeks Island salt remains essentially unchanged from that for WIPP clean salt.

The workhardening parameter,  $\Delta$ , is defined as the intercept on the ordinate axis of the logarithmic plot of strain rate verses the total strain. (Although it looks similar to Figure 2, the strain plot is a more sensitive and accurate method of determining the workhardening parameter). The workhardening data for Weeks Island salt are plotted in Figure 6 in comparison to the pure WIPP salt data. Based on Figure 6, to obtain a slightly better fit to the data, it would be acceptable to change the workhardening equation parameter constants, however, it hardly seems justified considering the scatter in the data. In addition, the exact value of this parameter is not especially critical. Thus, even though there is some considerable scatter, the data comparison suggests that the Weeks Island data are in reasonable agreement to the WIPP data.



T/M-10282-8

Figure 5. Transient Strain Limit Weeks Island and WIPP Salt [Munson and Ehgartner, 1997].

We must comment on the remainder of the M-D model parameters, even though they cannot be evaluated from the current database. As noted previously, most of these constants are independent of the exact salt material being considered. This results from the fact that many of these parameters are related to the salt physical properties and processes at an atomic level. The activation energies,  $Q$ , are related to atomic diffusion processes and, therefore, are not physically

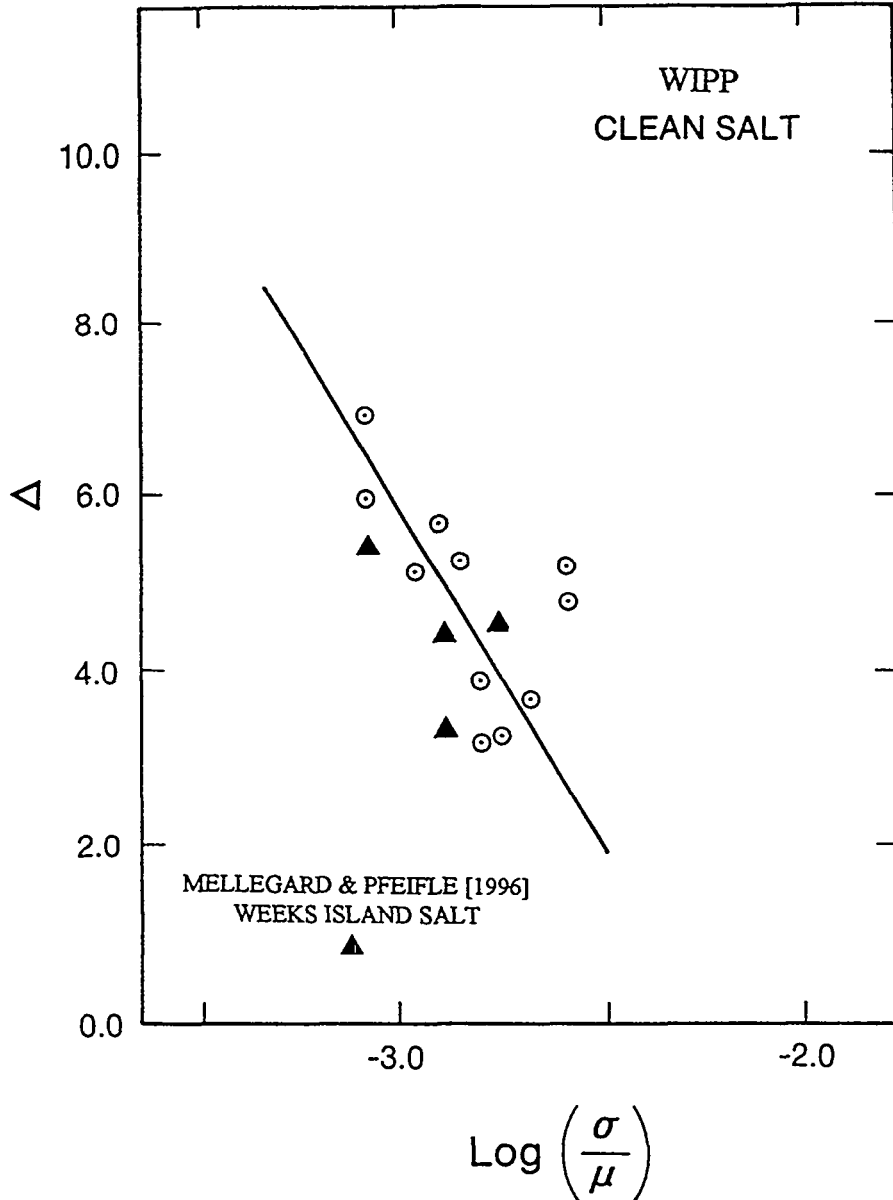


Figure 6. Workhardening of Weeks Island and WIPP Salt [Munson and Ehgartner, 1997].

sensitive to the origin differences of the various salt materials. Similarly, the stress exponents,  $n$ , are also related to local atomic processes and are insensitive to different salt materials. In this case we can be quite certain based on the physical models that describe them that the values of these parameters do not change. As a result, the same values of  $Q$ 's and  $n$ 's that were determined for WIPP clean salt will be used for Weeks Island salt, and for the other domal salts, as well. Values of the stress limit,  $\sigma_0$ , and the stress constant,  $q$ , are not, in general, sensitive to the salt material, although they may be. As a consequence, the values of these parameters,  $\sigma_0$  and  $q$ , from the WIPP

clean salt will be used for Weeks Island and the other domal salts. The value of  $m$  is a theoretical constant, independent of material. The non-critical value of  $c$  is related to an activation process and is assumed to remain unchanged with different materials. The parameter values determined for the Weeks Island salt are given in Table I, where the factor ( $A_{\text{DOMAL}}/A_{\text{WIPP}}$ ) is the vertical offset multiplier (or the  $\log_{10}$  difference) of the steady state compared to the WIPP baseline.

Table I. Structure Factor Multiplication Factor from WIPP 25°C Pure Salt Baseline.

Temp.	Factor	Clean		Soft Salt				Hard Salt		
		WIPP	AI*	WI	MB	WH	BH	BM	BC	JD
25°C	Multiplier	1.0	0.71	0.59	1.0	1.23	1.51	0.17	0.17	0.17
	Log <sub>10</sub> Differ.	0.00	-0.14	-0.23	0.00	+0.09	+0.18	-0.76	-0.77	-0.77

\* Because  $A_1$  could be evaluated directly, this factor applies to  $A_2$  only.

The Avery Island (AI) dome is one of a series of domes formed along the Gulf Coast from the ancient Luann salt formation. As such, it has many similarities with the other domal salts treated in this paper. The dome has been mined over the many decades since shortly after the Civil War, with several different mine operators during its long history. Initiation of both the Office of Nuclear Waste Isolation (ONWI) programs for disposal of civilian reactor waste and the WIPP program for disposal of defense generated nuclear waste resulted in the use of the Avery Island Mine for early underground studies in 1979. These studies were in anticipation of disposal of radioactive wastes in other geologic salt domes or formations [Ewing, 1981; Mellegard, 1983]. In addition to underground experiments, the mine also became a source of material for laboratory specimens. A number of cores were taken from the floor of a room at the 274 m (900 ft) mining level to provide specimen stock for testing [Mellegard, 1983]. Specimen stock was unusually clean, typically better than 98% salt, with minor amounts of anhydrite and argillaceous (clay) material at the grain boundaries.

From these cores, specimens were prepared for creep testing. Results of these tests have been presented in a number of reports, primarily with analyses to obtain parameters for several constitutive models being considered by ONWI, with an eye to selecting the best model [Senseny, 1983; DeVries, 1988]. DeVries [1988] determined the parameters for these models, including the M-D model, using a statistical software procedure developed for fitting biomedical research data. Although a set of parameter values was obtained for the M-D model using this procedure, the results are basically incompatible with the micromechanical aspects of the model. The specimens for laboratory creep testing were 100 mm (3.94 inch) in diameter. The tests were essentially all conventional creep tests under conditions of confined compression. There were eventually a total of 55 tests for which the deformation-time results were reported [DeVries, 1988].

The database for the Avery Island salt dome is extensive and permits the evaluation of all of the M-D model parameters directly. Unfortunately, because of space limitations here, the plots used to determine the parameters for Avery Island, and indeed all of the remaining domal salt materials, cannot be shown, with one exception, which illustrates the incremental tests. As a consequence, only the final results of the earlier analysis will be given, which is usually just the steady state



evaluation of the  $A_2$  parameter, as tabulated in Table I. The complete analysis, including the reported increment creep rates and graphical representations can be found in Munson [1998].

Using our analysis methodology, Avery Island salt at 25°C creeps somewhat slower than the WIPP baseline, with a multiplication factor of 0.71 (log -0.149). Appropriate intercept values for two mechanisms are given as  $6.869 \times 10^{+12}$  for  $A_2$  and  $1.137 \times 10^{+22}$  for  $A_1$ . Intercept values (B's) for the third, high stress, mechanism can not be determined directly so they are estimated by proportion between the first two mechanisms and the WIPP baseline.

Transient strain limits for the Avery Island salt are determined from the 25°C data and are consistent with the required WIPP baseline slope of 3, but are offset upward to give an intercept  $K_0$  of  $1.342 \times 10^{+6}$ . This indicates that Avery Island salt exhibits significantly greater transient strain than WIPP clean salt. The experimental values of  $\Delta$  are not inconsistent with slope of the WIPP baseline data, but are offset to higher values of  $\Delta$ . Appropriate  $\alpha$  and  $\beta$  parameter values are determined on this basis. Although the results are not shown here, the Avery Island data substantiate the activation energies determined from a typical Arrhenius plot for the WIPP baseline salt.

#### ANALYSIS OF INCREMENTAL TESTS FOR OTHER DOMAL SALTS

Six domal salts have been tested using incremental tests. These are Bryan Mound (BM), Big Hill (BH), Bayou Choctaw (BC), and West Hackberry (WH) domes that contain SPR facilities, and Moss Bluff (MB) and Jennings (JD) domes for which data are available.

Geologic structure of the Bryan Mound (BM) dome has been reported by Neal, et al. [1994]. The Bryan Mound specimens were prepared from stock that was obtained from coring of the same deep holes eventually used for solutioning. The specimens had a grain size range from 2 mm (0.08 inch) to 40 mm (1.6 inch), with an average grain size of about 8 mm (0.3 inch). The core also exhibited high angle dark bands or concentrations of anhydrite. Anhydrite concentration determined from a limited dissolution analysis was given as about 6 %.

Bryan Mound was studied in two different efforts. The earlier study [Wawersik, et al., 1980a] involved four separate specimens, three of which were tested using a conventional creep method. The remaining specimen was used for a bilevel incremental test in which the stress level was increased once. Sources of this earlier specimen material were Well 107A and Well 107C. In the later study [Wawersik and Zeuch, 1984], six specimens cored from deep boreholes were tested. Material was again primarily from Well 107C, with single specimens each from Well 108B and Well 113B. These specimens were tested using the incremental testing procedure in both stress and temperature. Although all of the specimens of the later study involved incremental testing, two specimens involved many, up to 14, separate increments and represent perhaps the extreme in incremental testing. The remaining four specimens tested had just a few (two or three) different increments. We have chosen to show the plot of the final increment strain rates for these four specimens in Figure 7. According to the analysis procedures, if we take the lower envelope of the rates as approaching the steady state rate, we can then construct the line parallel to the WIPP clean salt baseline data. This was done for the 60°C data in the figure and is shown as the dashed line. A similar line could be constructed for the other temperatures. The 60°C data are offset from the 22°C data by a factor of 3.16 (log +0.50), compared to a calculated factor of 5.89 (log +0.77) and the 100°C data are offset by a factor of 25.12 (log +1.40) compared to a calculated factor of 29.51 (log +1.47). While not exact, the relative temperature data are in reasonable conformance to the model predictions. However, in contrast the comparison to the WIPP clean salt baseline indicates the apparent steady state response for the 60°C Bryan Mound data is offset by a factor of about

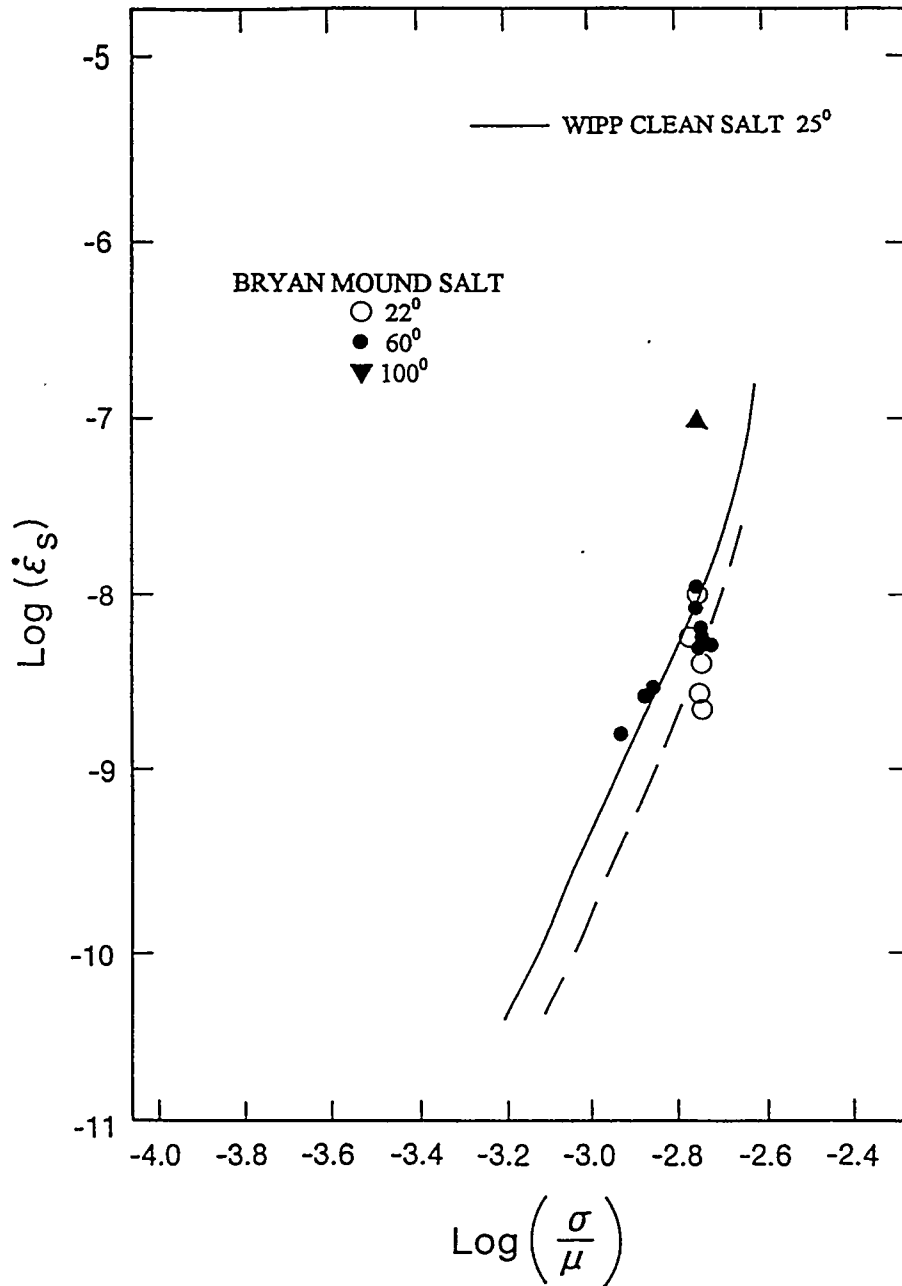


Figure 7. Incremental Test Final Rates Bryan Mound [data Wawersik and Zeuch, 1984].

0.05 (log -0.30) from the baseline data, while the 22°C data are offset by about a factor of 0.17 (log -0.78) from the baseline. This supports the contention that Bryan Mound salt is much more creep resistant, as was initially noted by Wawersik, et al. [1980a]. Again, this result is reflected by the multiplication factor in Table I.

The database for Big Hill (BH) salt is developed using stress and temperature change tests from three specimens [Wawersik, 1985]. The specimens were prepared from recovered core from two deep boreholes at the site, specifically Well 106B and Well 108B. Grain sizes were from medium to quite large, ranging from 3.7 mm (0.12 inch) to 51 mm (2.0 inch), with some grains in excess of 100 mm (4.0 inch) in diameter. Although the salt purity was probably high, visual examination suggested finely distributed anhydrite crystals in the specimens from Well 106B. Magorian and Neal [1988] described the geology of the site, and give a calculated median value of insolubles of 1.7%, probably anhydrite.

During the analysis, it was found that the 60°C Big Hill data are offset by a factor of 8.91 (a logarithmic value of +0.95), which is in excess of the expected temperature correction factor of 5.89 (log +0.77) by the amount of a factor of 1.5 (log +0.18). As a result, when all of the steady state creep rate of Big Hill are taken into account, the creep rate at 25°C appears to be somewhat greater than that of WIPP pure salt, and indeed also greater than that of Weeks Island salt. If the bounding envelope of data is indeed steady state, although there is no assurance of this from incremental test data, then the suggested multiplication factor is as stated. The limited creep data from Big Hill does not permit evaluation of the other creep parameters.

General studies of the West Hackberry (WH) dome as reported by Magorian, et al. [1991] essentially concentrated on the geologic characteristics. Two separate studies of the creep of West Hackberry domal salt have been reported. In an early study, Wawersik, et al. [1980b] studied a total of four specimens prepared from core take from the deep borehole of Well 6C. These specimens were tested in conventional creep tests. Dissolution tests on three separate core specimens gave an insoluble impurity content of 2.7 +/- 0.9 %, primarily anhydrite. The impurities seemed to be in bands through the specimens. The grain size was from 6 mm (0.25 inch) to 30 mm (1.2 inch). The creep rates of West Hackberry salt at 22°C and 60°C are essentially identical to the baseline WIPP clean salt data, at least within the typical scatter. This conclusion was supported by results of a later incremental test study [Wawersik and Zeuch, 1984] involving two additional West Hackberry domal salt specimens prepared from the core taken from Well 108.

One specimen was prepared from core recovered from deep Borehole 2 at the Moss Bluff (MB) dome [Wawersik, 1992]. Although an incremental test procedure was used, none of the incremental changes were stress drops. The average grain size of the specimen was 11 mm (0.4 inch). There was no indication of impurity content. The final creep rates for each of the increments suggest the response at 60°C is offset by a factor of about 5.62 (log +0.75) from the baseline WIPP clean salt data. This is consistent with the calculated temperature shift of a factor of 5.89 (log +0.77). Although there is some uncertainty in the data for other temperatures, we will assume that the 60°C data are the correct response. As a result, Moss Bluff salt steady state creep is essentially identical to the WIPP clean salt baseline data.

Neal, et al. [1993b] analyzed the geology of the Bayou Choctaw (BC) dome. Core taken from Well 101 at intervals down to a depth of 728 m (2390 ft) was clear with 10 to 20 mm (0.4 to 0.8 inch) diameter grains, and 1 mm (0.04 inch) gray anhydrite bands. Core from the same well at a depth of 1446 m (4743 ft) was black with 5 mm (0.2 inch) crystals and about 5 % anhydrite in wavy bands.

The creep response from one specimen of Bayou Choctaw salt prepared from core obtained from Well 19A was determined using the incremental stress and temperature change procedure [Wawersik and Zeuch, 1984]. Unfortunately, the incremental tests involved several stress drops. If the stress drop increment results are eliminated, the 60°C minimum data are essentially identical to the 25°C WIPP clean salt baseline. The 80°C data are consistent, being offset somewhat above the 22°C Bayou Choctaw test results. As a consequence, the Bayou Choctaw material appears to be more creep resistant than the WIPP clean salt by about a factor of 0.17, and consequently has a very similar creep response to that of Bryan Mound.

A single specimen take from the deep borehole LA-1 at the Jennings dome (JD) was tested using the stress and temperature increment procedure [Wawersik and Zimmerer, 1994]. No information is available on specimen grain size or on impurity content. The data involves only one stress drop, which we do not consider. The remaining 60°C Jennings Dome data agree well with 25°C WIPP clean salt baseline, which indicates the Jennings Dome salt has a greater creep resistance, again by about a factor of 0.17.

## DISCUSSION

Our analysis of the creep of the domal salts indicates that the well-defined creep tests on Avery Island and Weeks Island salt produce essentially the same constitutive behavior as the WIPP clean salt, with only changes in parameter values. As a result, the M-D model appears to be an adequate description of domal salts. Extending this concept, the forms suggested by the model can be used to determine the possible steady state response envelope from the less well defined creep data of a number of materials from other salt domes. In addition to conventional creep tests, these materials were often tested using incremental stress and temperature change methods that require an analysis based on an understanding of transient creep response. Under certain circumstances, all these tests can lead to a definition of the steady state creep behavior. Because all of the creep tests were conducted at relatively low stress and low temperature, we can characterize the creep in terms of the structure factor of just one of the three mechanisms involved in salt creep. This is the undefined or empirical mechanism with the structure factor  $A_2$ . Values of the structure factor can be used to evaluate the relative creep "resistance" of the various domal salts compared to the WIPP clean salt creep baseline. In the discussion of individual creep data, the analysis of the domal salt creep data used temperature-corrected offsets to determine the most probable equivalent 25°C-creep response. The 25°C equivalent offset amounts are summarized in Table I.

In discussing the results of our analysis, one must remember that the database for any given salt material is very sparse and often further confused by experimental peculiarities. These facts leave considerable room for error in interpretation. As a result, no firm statements are currently possible, even though we will deduce some possible conclusions. It appears from the table that not only is there some variation between the individual results, but also there are two relatively distinct groups of salt. Four domal salts fall within the expected experimental uncertainty (about a factor of 2, or  $\log_{10}$  difference of +/- 0.30) of the WIPP clean salt behavior. These salts are probably experimentally indistinguishable. However, three of the domal salts apparently fall beyond the uncertainty and form a distinct group of more creep resistant materials.

Indirect substantiation of the effect of differences in the creep response of domal salt is found in the work of Ehgartner, et al. [1995] on loss of volume of petroleum storage caverns of the SPR. These results are produced from a CAVEMAN simulation methodology based on the M-D creep equations. The methodology generates a set of "effective" fitting parameters for material, geometry, pressurization, and stress in the cavern setting as determined from cavern pressurization and fluid withdrawal histories and can be used to predict "effective" SPR cavern creep rates.

These rates have been recently reported [Ehgartner attachment in Linn, 1997 ] from an ullage study. The effective creep rates in volume loss percentage per year (the same as a linear rate) are shown in Figure 8. Of the four facilities studied, Big Hill and West Hackberry show the highest creep volume loss rates; whereas, Bryan Mound and Bayou Choctaw show the lowest creep volume loss rates.

The reported volume creep rates certainly agree with the results suggested by Table I. We would expect the cavern response to follow the laboratory creep responses. However, the volume loss results also suggest that the Bryan Mound dome must contain two different salt types. Most of the caverns of Bryan Mound exhibit relatively small closure rates associated with the creep resistant salts, whereas Caverns BM 113, BM 114, BM115, and BM116 exhibit greater volume creep closure rates comparable to higher closure rates of the Big Hill and West Hackberry caverns.

Why some apparently high purity salts have greater creep resistance than other high purity salts is not known. Interestingly, the differences do not appear to form a continuous function with a gradation of behavior between the extremes. Rather, the effect seems discontinuous. Since most secondary strengthening agents, such as grain size, impurity contents, or second phase quantities lead to continuous changes, it is not satisfying to suggest simply that micromechanical agents lead to the observed behavior.

By applying ratios determined from the creep results, we can establish some suggested M-D creep parameters. However, the limited database permits only structure factors to be determined; all other parameters must be established on the basis of the WIPP clean salt database and the logical extension of the WIPP parameters, considering how material variation can affect the parameter. These results are given in Table II for WIPP clean salt, Weeks Island salt, the hard domal salts, and the soft domal salts. Those underlined quantities are extensions of WIPP parameter values based on theoretical values, micromechanical model parameter values, or atomistic models. The only parameter value that has no basis in the experimental data or a logical extension, and is therefore an assumed value, is the value of  $K_0$ , which may indeed depend strongly upon specific salt material. These assumed values are in parentheses in the table. Unless more experimental information becomes available,  $K_0$  will be taken as either the WIPP clean salt value ( $6.275 \times 10^{+5}$ ), as given in Table II, or the WIPP argillaceous salt value ( $1.783 \times 10^{+6}$ ), depending upon the impurity content of the domal salt. When one suspects that a given domal salt is acting similar to argillaceous salt, it may also be necessary to reconstruct the table using the WIPP argillaceous parameters as a baseline material. Except for  $K_0$ , the argillaceous creep parameters differ only slightly from the clean salt parameters. The argillaceous parameters are not repeated here, but can be found elsewhere [Munson, 1997].

## CONCLUSIONS

The limited databases on salt creep from experimental studies of material from several salt domes, including the five SPR facility sites, have been analyzed using the procedures prescribed for the M-D model of salt creep. The M-D model was developed for the WIPP project. Even though the database information is limited, the parameter values for each domal salt have been established on the basis of the experimental data, theoretical values, material based extensions, or reasonable assumptions. Sufficient creep data are available from one SPR site (Weeks Island) and for Avery Island salt to indicate that they are consistent with the M-D model and the WIPP clean salt baseline. When all data are compared to the WIPP clean salt baseline response, there appear to be two types of materials: a creep resistant or hard salt and a soft salt with creep similar to the baseline material. In fact this has made it possible to generate Table II of suggested M-D model parameters based on this analysis. These parameters are now available for potential future use in

Table II. Suggested Parameter Values for the M-D Model.

Type→	Salt				
	Baseline WIPP	WI	AI	Soft BH, WH, MB	Hard BM, BC, JD
Ave. Factor→	1.00	0.59	0.71	~1.17	~0.17
<hr/>					
<u>Parameter</u>					
$\mu$ GPa	12.4				
E GPa	31.0				
$\nu$	0.25				
$A_1$ 1/s	<b>8.386<sub>5</sub>x10<sup>+22</sup></b>	4.948x10 <sup>+22</sup>	1.137x10 <sup>+22</sup>	9.812x10 <sup>+22</sup>	1.445x10 <sup>+22</sup>
$Q_1$ (Cal/mol)	<b>25</b>	<u>25</u>	25	<u>25</u>	<u>25</u>
$n_1$	<b>5.5</b>	<u>5.5</u>	5.5	<u>5.5</u>	<u>5.5</u>
$B_1$ 1/s	<b>6.086x10<sup>+6</sup></b>	5.417x10 <sup>+6</sup>	0.825x10 <sup>+6</sup>	7.121x10 <sup>+6</sup>	1.049x10 <sup>+6</sup>
$A_2$ 1/s	<b>9.672x10<sup>+12</sup></b>	<b>5.706x10<sup>+12</sup></b>	6.869x10 <sup>+12</sup>	11.32x10 <sup>+12</sup>	1.667x10 <sup>+12</sup>
$Q_2$ (Cal/mol)	<b>10</b>	<u>10</u>	10	<u>10</u>	<u>10</u>
$n_2$	<b>5.0</b>	<u>5.0</u>	5.0	<u>5.0</u>	<u>5.0</u>
$B_2$ 1/s	<b>3.034x10<sup>-2</sup></b>	2.700x10 <sup>-2</sup>	2.155x <sup>10-2</sup>	3.550x10 <sup>-2</sup>	0.523x10 <sup>-2</sup>
$\sigma_0$ MPa	<b>20.57</b>	20.57	20.57	20.57	20.57
q	<b>5.335x10<sup>+3</sup></b>	5.335x10 <sup>+3</sup>	5.335x10 <sup>+3</sup>	5.335x10 <sup>+3</sup>	5.335x10 <sup>+3</sup>
m	<b>3.0</b>	<u>3.0</u>	<u>3.0</u>	<u>3.0</u>	<u>3.0</u>
$K_0$	<b>6.275x10<sup>+5</sup></b>	<b>6.275x10<sup>+5</sup></b>	1.342x10 <sup>+6</sup>	(6.275x10 <sup>+5</sup> )	(6.275x10 <sup>+5</sup> )
c	<b>0.009198</b>	0.009198	0.009198	0.009198	0.009198
$\alpha$	<b>-17.37</b>	-17.37	-13.20	-17.37	-17.37
$\beta$	<b>-7.738</b>	-7.738	-7.738	-7.738	-7.738
$\delta$	<b>0.58</b>	0.58	0.58	0.58	0.58
$\omega$	0.0	0.0	0.0	0.0	0.0

Bold numbers are determined from creep data for that specific salt dome material.

Underlined values are theoretical micromechanism constants and are the same as WIPP clean salt values.

$K_0$  values in parentheses are assumptions.

All other values are assumed to be the same as the WIPP salt values or adjusted from the WIPP salt value in proportion to the  $A_2$  value obtained experimentally for each individual domal salt, except for Avery Island salt where  $A_1$  can be determined directly.

Because the Multimechanism Deformation (M-D) model is used, the equations given in this report require a zero value of  $\omega$ .

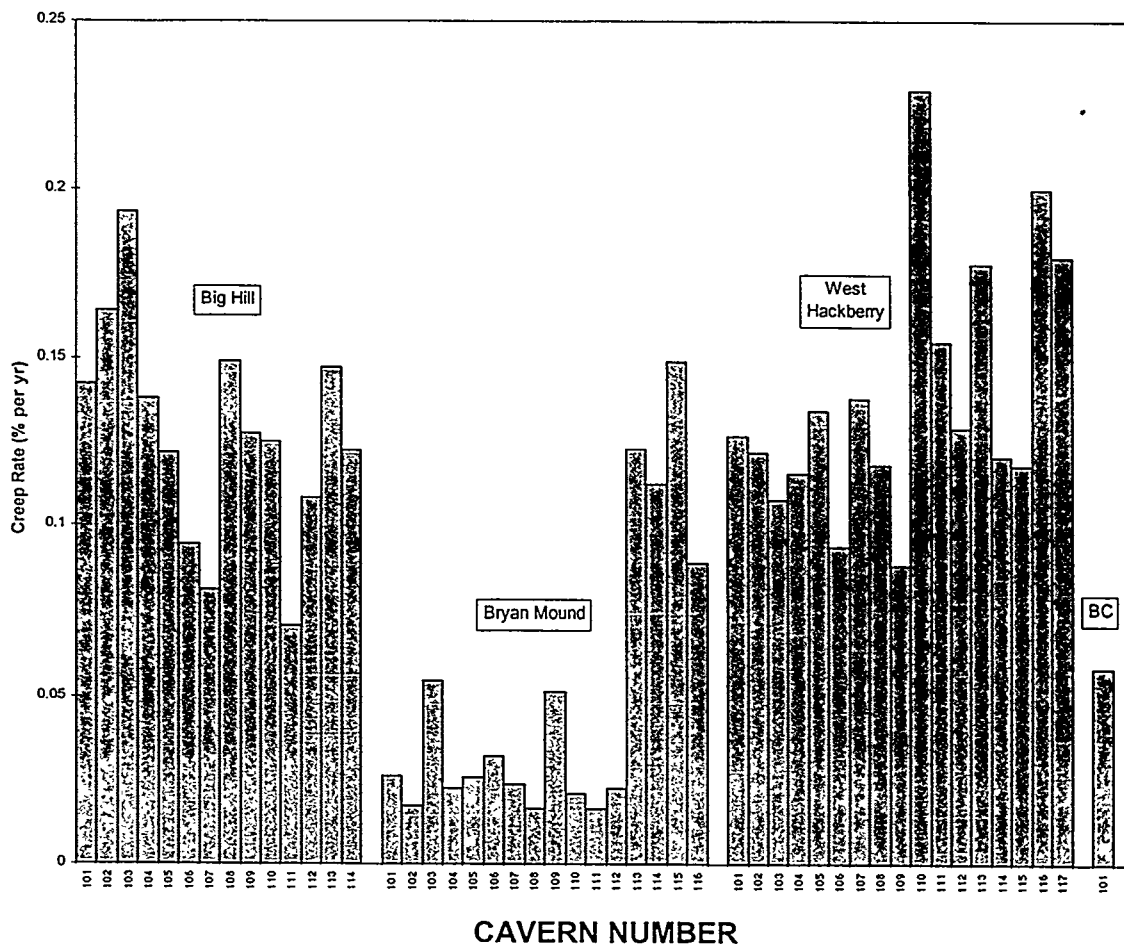


Figure 8. Caveman Volume Creep Rates for SPR Caverns [Ehgartner attachment in Linn, 1997].

prediction of cavern behavior through the use of the M-D model and the appropriate numerical simulation methods. These numerical techniques have become a significant tool in examining the behavior of underground openings in salt.

Perhaps the most significant result of the analysis is the potential for a limited number of creep tests on core obtained from potential cavern sites to give a good prediction of the cavern volume creep behavior. This has always been suspected to be the case, however, the potential is clearly demonstrated in this work and indicates the very interesting possible utilization of the available technology to anticipate cavern behavior before construction.

## REFERENCES

- DeVries, K.L., 1988. Viscoplastic Laws for Avery Island Salt, Report for Stone Webster, RSI-0333, RE/SPEC, Inc., Rapid City, SD.
- Ehgartner, B., S. Ballard, M. Tavares, S. Yeh, T. Hinkebein, and R. Ostensen, 1995. A Predictive Model for Pressurization of SPR Caverns, Proc. Fall Meeting 1995, San Antonio, TX, Solution Mining Research Institute, Deerfield, IL.
- Ewing, R. I., 1981. Test of a Radiant Heater in the Avery Island Salt Mine, SAND81-1305, Sandia National Laboratories, Albuquerque, NM.
- Linn, J.K., 1997. Letter to R.E. Myers, November 25, 1997 with attachment on "SPR Ullage Study" by B.L. Ehgartner, Sandia National Laboratories, Albuquerque, NM.
- Magorian, T.R., and J.T. Neal, 1988. Strategic Petroleum Reserve (SPR) Additional Geologic Site Characterization Studies Big Hill Salt Dome, Texas, SAND88-2267, Sandia National Laboratories, Albuquerque, NM.
- Magorian, T.R., J.T. Neal, S. Perkins, Q.J. Xiao, and K.O. Byrne, 1991. Strategic Petroleum Reserve (SPR) Additional Geologic Site Characterization Studies West Hackberry Salt Dome, Louisiana, SAND90-0224, Sandia National Laboratories, Albuquerque, NM.
- Mellegard, K.D., 1983. Quasi-Static Strength and Creep Characteristics of 100-mm-Diameter Specimens of Salt from Avery Island, Louisiana, Technical Report ONWI-250, Office of Nuclear Waste Isolation, Battelle, Columbus, OH.
- Mellegard, K.D., and T.W. Pfeifle, 1996. Laboratory Creep test on Domal Salt from Weeks Island, Louisiana, Topical Report RSI-0756, RE/SPEC Inc., Rapid City, SD.
- Munson, D.E., 1979. Preliminary Deformation-Mechanism Map for Salt (with Application to WIPP), SAND70-0079, Sandia National Laboratories, Albuquerque, NM.
- Munson, D.E., and P.R. Dawson, 1982. A Transient Creep Model for Salt during Stress Loading and Unloading, SAND82-0962, Sandia National Laboratories, Albuquerque, NM.
- Munson, D.E., A.F. Fossum, and P.E. Senseny, 1989. Advances in Resolution of Discrepancies between Predicted and Measured In Situ WIPP Room Closures, SAND88-2948, Sandia National Laboratories, Albuquerque, NM.
- Munson, D.E., 1997. Constitutive Model of the Creep of Rock Salt Applied to Underground Room Closure, Int'l. J. Rock Mech. and Min. Sci. & Geomech. Abstr., 34 (2), 233-248.
- Munson, D.E., and B.L. Ehgartner, 1997. Memorandum to J.K. Linn, July 11, 1997. "Comparison of Steady State Creep Response of Weeks Island and WIPP Salt," Sandia National Laboratories, Albuquerque, NM.
- Munson, D.E., 1998. Analysis of Multistage and Other Creep Data for Domal Salts, SAND98-2276, Sandia National Laboratories, Albuquerque, NM.



- Neal, J.T., T.R. Magorian, R.L. Thoms, W.J. Autin, R.P. McCulloh S. Denzler, and K.O. Byrne, 1993a. Anomalous Zones in Gulf Coast Salt Domes with Special Reference to Big Hill, TX, and Weeks Island, LA, SAND92-2283, Sandia National Laboratories, Albuquerque, NM.
- Neal, J.R., T.R. Magorian, K.O. Byrne, and S. Denzler, 1993b. Strategic Petroleum Reserve (SPR) Additional Geologic Site Characterization Studies Bayou Choctaw Salt Dome, Louisiana, SAND92-2284, Sandia National Laboratories, Albuquerque, NM.
- Neal, J.R., T.R. Magorian, and S. Ahmad, 1994. Strategic Petroleum Reserve (SPR) Additional Geologic Site Characterization Studies Bryan Mound Salt Dome, Texas, SAND94-2331, Sandia National Laboratories, Albuquerque, NM.
- Ortiz, T.S., 1980. Strategic Petroleum Reserve (SPR) Geological Summary Report Weeks Island Salt Dome, SAND80-1323, Sandia National Laboratories, Albuquerque, NM.
- Pfeifle, T.W., T.J. Vogt, and G.A. Brekken, 1996. Correlation of Chemical, Mineralogic, and Physical Characteristics of Gulf Coast Dome Salt to Deformation and Strength Properties, Proc. Solution Mining Research Institute, Spring Meeting, Houston, TX. pp. 221-254.
- Senseny, P.E., 1983. Review of Constitutive Laws used to Describe the Creep of Salt, ONWI-295, Office of Nuclear Waste Isolation, Battelle Memorial Institute, Columbus, OH.
- Senseny, P.E., 1983. Non-Associated Constitutive Laws for Low Porosity Rocks, Int'l J. Numerical and Analytical Methods in Geomechanics, 7, 101-115.
- Senseny, P.E. 1986. Triaxial Compression Creep Tests on Salt from the Waste Isolation Pilot Plant, SAND85-7261, Sandia National Laboratories, Albuquerque, NM.
- Senseny, P.E., 1989. Published as: Senseny, P.E., 1990. Creep of Salt from the ERDA-9 Borehole and the WIPP Workings, SAND79-0076, Sandia National Laboratories, Albuquerque, NM.
- Wawersik, W.R., D.J. Holcomb, D.W. Hannum, and H.S. Lauson, 1980a. Quasi-Static and Creep Data for Dome Salt from Bryan Mound, Texas, SAND80-1434, Sandia National Laboratories, Albuquerque, NM.
- Wawersik, W.R., D.W. Hannum, and H.S. Lauson, 1980b. Compression and Extension Data for Dome Salt from West Hackberry, Louisiana, SAND79-0688, Sandia National Laboratories, Albuquerque, NM.
- Wawersik, W.R., and D.H. Zeuch, 1984. Creep and Creep Modeling of Three Domal Salts – A Comprehensive Update, SAND84-0568, Sandia National Laboratories, Albuquerque, NM.
- Wawersik, W.R., 1985. Memorandum to R.R. Beasley, January 3, 1985, “Creep Measurements on Big Hill Salt,” Sandia National Laboratories, Albuquerque, NM.
- Wawersik, W.R., 1992. Indicator Tests for the Creep of Rock Salt from Borehole Moss Bluff 2, Moss Bluff Dome, Texas, SAND92-2122, Sandia National Laboratories, Albuquerque, NM.
- Wawersik, W.R., and D.J. Zimmerer, 1994. Triaxial Creep Measurements on Rock Salt from the Jennings Dome, Louisiana, Borehole LA-1, Core #8, SAND94-1432, Sandia National Laboratories, Albuquerque, NM.